 doi:10.20944/preprints201808.0302.v1

Effects of changes in soil hydraulic properties after crop abandonment on co-occurring perennial species in a semi-arid grassland in Mongolia

Aki Yanagawa[1]*, Haruyuki Fujimaki[2], Undarmaa Jamsran[3], Toshiya Okuro[4], Kazuhiko Takeuchi[4]

[1] Meisei University, Department of Environmental Systems and Engineering, 2-1-1 Hodokubo, Hino, Tokyo 191-8506, Japan

[2]The Division of Appropriate Technology and Science for Sustainable Development, Graduate School of Life and Environment Sciences, Tottori University, 1390 Hamasaka, Tottori 680-0001, Japan

[3]Center for Ecosystem Study, Mongolian State University of Agriculture, 210153 Ulaanbaatar, Mongolia

[4] Graduate School of Agricultural and Life Sciences, The University of Tokyo, 1-1-1 Yayoi, Bunkyo-ku, Tokyo 113-8657, Japan

*Corresponding author

Tel: +81- 42-591-6212

E-mail: aki.yanagawa@meisei-u.ac.jp

 doi:10.20944/preprints201808.0302.v1

Abstract

The objective of this study was to investigate successional changes in water flow as a result of changes in soil hydraulic properties after crop abandonment under drought and non-drought conditions, and under water uptake by co-occurring perennial plant species to clarify the observation that typical perennial grass species are seldom observed in abandoned fields. Soil hydraulic properties were measured in croplands which had been abandoned for different periods (2, 9, and 18 years from abandonment) and in a grazed grassland site. Hydrological processes in the soil profiles were simulated with soil hydraulic properties under drought and non-drought summer conditions with water uptake from perennial grass species Suction in the surface soils increased with the period of abandonment, with this trend being particularly obvious in a drought year. Available water appears to be restricted in the later successional stage of abandoned fields and in grazed grassland for plants that have drought tolerance. Dry soil and climate conditions are important factors determining the intrusion of the typical perennial grass, *S. krylovii*, into degraded abandoned fields. This abiotic interaction between soil hydraulic properties and climate conditions may play an important role for plant succession in abandoned cropland.

Keywords: unsaturated hydraulic conductivity, water restoration, cumulative transpiration, particle size distribution, grazed grassland

 doi:10.20944/preprints201808.0302.v1

Introduction

Crop abandonment is a factor responsible for soil degradation in semi-arid regions. Soil degradation within a few decades following abandonment of cropping is a serious problem in Mongolia and Inner Mongolia [1,2]. The dominant land use in these areas is grazing. Palatable grasses for livestock are originally dominant. Grasslands are dominated by the perennial grass, *Stipa krylovii*, which has lower vulnerability for drought than degraded grassland where annual species dominate [3]. However, the dominant species of typical perennial grasslands are seldom found in abandoned fields in Mongolia, even decades after abandonment [1] and in Inner Mongolia [4]. Instead of typical perennial species, annual species and the perennial species (*Leymus chinensis*), which has a high compensation rate, tend to dominate such grasslands [1,4].

Active ecological restoration has been tried in Mongolia to accelerate the recovery process. For instance, sowing of typical perennial grasses [5] and making gaps by removal of annual species [6] in abandoned fields have been tried. However, these activities have not brought the expected results due to unexpected drought and degraded soil conditions [5,6]. These limitations of restoration activities may result from having inappropriate particular goals or from targeting apparent symptoms without considering underlying causes [7]. Therefore rigorous assessment of the state of abandoned cropland in the Mongolian rangeland and the underlying factors leading to that state, such as changes in soil hydraulic properties and plant species composition under annual variability of precipitation, should be undertaken as a first step in restoration activity.

The effects of crop abandonment on soil restoration may depend on soil properties and climatic conditions of an area [8]. In particular, soil hydraulic properties affect the vegetation recovery process [9]. Soil water suction interacts with water uptake by plant roots. Therefore, measuring the changes in average suction after crop abandonment is critical in understanding soil water conditions for typical perennial plant growth. Previous studies have found changes in particle size distribution [1,10,11], hydraulic properties of the near-saturated range of surface and subsurface soils [12,13] and unsaturated hydraulic conductivity (i.e., high suction range) of surface soils [1] due to crop abandonment in the semi-arid region. However, there are insufficient studies on successional changes in infiltration into and capillary rise from the subsoil that occur when considering the changes in unsaturated hydraulic properties after crop abandonment. In addition to changes in hydraulic properties of the soil profile, there is substantial annual variability in climatic conditions in semi-arid regions. Therefore it is important to investigate soil hydraulic properties under various climatic conditions when evaluating the soil water condition in places where typical perennial species grow to answer the question as to why typical perennial species such as *S. krylovii* have seldom been observed in abandoned cropland.

The objective of this study is to present the successional changes in water flow due to changes in the soil hydraulic properties after crop abandonment under drought and non-drought conditions, and under water uptake by co-occurring dominant plant species to clarify the reason why typical perennial grass species are seldom observed in abandoned fields.

Materials and methods

Study site and soil sampling

The study area was in Hustai National Park (HNP, 47°50′N, 106°00′E) in Mongolia. The average elevation of HNP is 1240 m asl. The climate of the region is semi-arid and cold, with short summers. Most of the annual precipitation falls in summer, from May to July, which is critical for the growth of plants. According to meteorological data from the HNP climatic station, annual precipitation was approximately 232 mm (C.V. 31%) and the mean annual temperature was approximately 0°C from 1999 to 2005 at HNP. The zonal soils were classified as Kastanozems by WRB [14] based on soil profile morphology and physicochemical properties.

All abandoned croplands had been tilled from 1977 in this area by administrative plan. Satellite images (Landsat MSS 1994, 1996, 1999, 2002, 2005, 2007) were used to confirm the period of abandonment. We then consulted municipal archives and held personal interviews with landowners to determine the period of abandonment. We selected croplands that had been abandoned in 1990 (site CA18), 1999 (CA9) and 2006 (CA2) and semi-natural grassland (SNG) in the flat buffer zone in Hustai National Park as a reference site. The CA2, CA9 and CA18 sites had been abandoned from cropping two, nine and eighteen years, respectively, prior to our survey in summer 2008. Wheat had been cultivated prior to the cropland being abandoned. The cropping system and agricultural materials (e.g. fertilizer and agricultural machines) used at each site basically followed the government guidelines until 1990. Although the abandoned cropland sites had had different durations of cultivation, previous studies reported that half of the changes in soil physicochemical properties occur during the first 8 years from primary tillage, and subsequent changes are slow [2,15]. All of the study sites of abandoned fields had been cultivated for more than 12 years. Hence, the study sites should allow proper comparison of the effects of crop abandonment on soil and plant properties between these sites. Grazing was introduced on all abandoned cropland sites after crop abandonment. Livestock numbers were strictly controlled by HNP in the buffer zone including CA2, CA9, CA18 and SNG.

Annual forbs (*Erodium stephanianum*, *Artemisia macrocephala*, *Chenopodium aristatum*) dominated at the CA2 site, annual forbs (*Erodium stephanianum*) and perennial grasses (*Leymus chinensis*) were growing at the CA9 site, perennial grasses (*Leymus chinensis*, *Cleistogenes squarrosa*) dominated at the CA18 site and perennial grasses (*Stipa krylovii*) and shrubs (*Kochia prostrata*) dominated at the SNG site. Since *S. kylovii* is replaced by *L. chinensis* when land degrades (Hilbig 1995), the dominant grass at SNG, *S. krylovii*, was not dominant in the abandoned fields.

Soil surveys and soil sampling were performed from July to August 2008. Soil cores (100 ml) were sampled from depths of 0–5, 10–15 and 30–35 cm in the three different fields to investigate the variation in each field. The selection of soil layers for sampling was based on the soil profile observations. The sampled soil cores did not contain the boundaries between soil horizons.

Preprints (www.preprints.org) | NOT PEER-REVIEWED | Posted: 17 August 2018 doi:10.20944/preprints201808.0302.v1

Calculations of plant growth and hydrological fluxes

Initial simulations of soil water flow were performed for the bare surface condition to focus on the effect of changes in soil hydraulic properties with different periods of crop abandonment and land-use history on average suction and volumetric water content. We then simulated the cumulative evaporation of the dominant two species (*Stipa krylovii* and *Leymus chinensis*) and water movement under those plants, to compare the effects of drought and differences in soil hydraulic properties on the growth of these two species. Since *S. krylovii* and *L. chinensis* were not observed at the CA2 site, we did not use the soil hydraulic properties of this site.

The various terms of water balance in one dimension were simulated using WASH_1D (http://www.alrc.tottori-u.ac.jp/fujimaki/download/WASH_1D/WASH_1D.zip), which solves the one-dimensional Richards' equation and convection-diffusion equation for heat movement with the finite difference method. The WASH_1D program considers the dependence of albedo on water content and vapor movement due to the thermal gradient and hysteresis. The potential evaporation rate was calculated by the Penman equation. A plant growth model is also involved in this program.

We simulated the soil water movement in the 0–5 cm, 5–15 cm and 15–50cm soil layers with core soil samples from the 0–5 cm, 10–15 cm and 30–35cm depths, respectively. Tables 1 and 2 show all parameter values for soil and plants, respectively.

Preprints (www.preprints.org) | NOT PEER-REVIEWED | Posted: 17 August 2018 doi:10.20944/preprints201808.0302.v1

Table 1 Parameter values of soil hydraulic properties in the hydrological simulation.

	CA2a			CA2b			CA2c			CA9a			CA9b			CA9c		
Simulated soil depth (cm)	2.5	12.5	40	2.5	12.5	40	2.5	12.5	40	2.5	12.5	40	2.5	12.5	40	2.5	12.5	40
Soil water retention curve																		
Wsat	0.445	0.478	0.386	0.433	0.399	0.43	0.449	0.456	0.447	0.475	0.498	0.446	0.467	0.39	0.559	0.53	0.531	0.526
Zeta	0.01	0.02	0.04	0.019	0.02	0.04	0.02	0.02	0.014	0.015	0.015	0.025	0.049	0.049	0.049	0.038	0.02	0.02
alpha	0.022	0.017	0.022	0.014	0.018	0.051	0.016	0.038	0.075	0.016	0.017	0.023	0.007	0.009	0.019	0.018	0.037	0.011
N	1.42	1.682	1.748	1.808	1.629	1.26	1.595	1.437	1.274	1.482	1.424	1.343	2.201	1.568	1.508	1.45	1.237	1.303
M	0.333	0.38	0.4	0.446	0.386	0.27	0.35	0.29	0.225	0.325	0.298	0.256	0.54	0.326	0.307	0.3	0.22	0.233
Hydraulic Conductivity																		
Ksat	0.003	0.003	0.006	0.002	0.004	0.002	9E-04	0.002	0.002	0.001	0.001	0.003	9E-04	2E-04	0.001	0.005	0.002	0.001
Ak	0	0	0	0	0	0	0	0	0	0	0	0	0	0	0	0	0	0
Bk	-0.26	0	0	-2.33	0	0	0	0	0	4.64	0	0	10.78	0	0	9.893	0	0
Ck	8.94	8.58	9.7	8.34	8.62	7.25	8.31	8.81	9.83	8.51	10.47	15.58	7.45	11.17	8.78	10.68	11.81	9.49
Thermal Conductivity																		
a_h	0.0061			0.0075			0.0071			0.0062			0.0062			0.0051		
b_h	0.0068			0.0065			0.0063			0.0057			0.0062			0.0062		
c_h	0.54			0.6369			0.3261			0.37			0.3556			0.4809		
d_h	0.0036			0.004			0.0039			0.0036			0.0036			0.0033		
e_h	4			4			4			4			4			4		
Albedo																		
Max	0.276	-	-	0.273	-	-	0.296	-	-	0.209	-	-	0.237	-	-	0.22	-	-
Min	0.209	-	-	0.18	-	-	0.19	-	-	0.169	-	-	0.186	-	-	0.179	-	-
a_al	0.15	-	-	10	-	-	8	-	-	4	-	-	16	-	-	5	-	-
b_al	2.4	-	-	3	-	-	1	-	-	5	-	-	2.27	-	-	1	-	-
Walb	1	-	-	1	-	-	1	-	-	1	-	-	1	-	-	1	-	-

Preprints (www.preprints.org) | NOT PEER-REVIEWED | Posted: 17 August 2018 doi:10.20944/preprints201808.0302.v1

Table1 Parameter values of soil hydraulic properties in the hydrological simulation. (*continued*)

	CA18a			CA18b			CA18c		
Simulated soil depth (cm)	2.5	12.5	40	2.5	12.5	40	2.5	12.5	40
Soil water retension curve									
Wsat	0.441	0.396	0.359	0.437	0.419	0.41	0.434	0.418	0.414
zeta	0.022	0.03	0.036	0.023	0.023	0.023	0.014	0.014	0.014
alpha	0.013	0.018	0.012	0.01	0.016	0.023	0.013	0.015	0.015
n	1.689	1.5	1.722	1.761	1.538	1.65	1.52	1.702	1.618
m	0.408	0.333	0.3	0.341	0.37	0.3	0.342	0.37	0.382
Hydraulic Conductivity									
Ksat	0.002	0.002	0.003	8E-04	0.002	0.003	7E-04	0.002	0.004
ak	0	0	0	0	0	0	0	0	0
bk	2.63	0	0	13.35	0	0	0.99	0	0
ck	8.45	12.16	10.92	6.8	9.92	8.65	9.79	9.24	10.34
Thermal Conductivity									
a_h		0.0075			0.0075			0.0068	
b_h		0.0066			0.0066			0.0061	
c_h		0.5			0.318			0.2819	
d_h		0.004			0.0041			0.0038	
e_h		4			4			4	
Albedo									
Max	0.207	-	-	0.232	-	-	0.211	-	-
Min	0.183	-	-	0.185	-	-	0.18	-	-
a_al	10	-	-	10	-	-	5	-	-
b_al	3	-	-	2	-	-	5	-	-
Walb	1	-	-	1	-	-	1	-	-

 doi:10.20944/preprints201808.0302.v1

Meteorological data

Meteorological data for precipitation, maximum and minimum temperatures, wind velocity, relative humidity, sunshine duration and direct radiation for every 3 h were used in the simulation. These data were obtained from the Institute of Meteorology and Hydrology (IMH) and World Radiation Data Centre in Tov Prefecture where HNP is located. Since we focused on soil hydraulic properties as the critical condition determining water availability for plants, the simulated period was restricted to the plant growth period (May–July). To reflect a typical climate difference, we selected data from non-drought (1999) and drought (2004) summers. Amounts of precipitation during the relevant periods were 158 and 81 mm, respectively. We assumed that the initial suction was uniform at 300 cm.

Soil hydraulic properties

Saturated hydraulic conductivity was measured by the falling head method for every soil core sample. Unsaturated hydraulic conductivity and retention data were measured by the evaporation method using two tensiometers [16]. Those at the surface layer were determined by an evaporation method, which gives hydraulic conductivity at a high suction (>600 cm) range. In this evaporation method, two tensiometers were used until suction at the upper tensiometer reached more than 500 cm. After removing the water in the tensiometers, the soil column was again placed under the evaporative condition until the evaporation rate became lesser than 10% of that at the initial stage. After termination, the soil columns were dismantled to obtain the water

 doi:10.20944/preprints201808.0302.v1

content profiles. Parameters in hydraulic conductivity functions in the high suction range were inversely determined using tensiometer readings, cumulative evaporation derived from the weight change of soil samples through the experiments and the water content profile in the objective function. The values for unsaturated hydraulic conductivity and retention curves were determined in this way and validated by comparison with unsaturated hydraulic conductivity and water retention data measured using the multi-step outflow experiment of Fujimaki and Inoue (2003)[17]. We further validated the method that we used with the known hydraulic properties of the Kanto loam. Retention data in the high suction range (14077 cm, 402941 cm) were obtained using the vapor pressure method for surface core samples because soil water suction covers a wide range in the semi-arid Mongolian grassland.

The water-retention data were fitted with a modified version of Shiozawa's equation:

$$\theta = \frac{\theta sat - \zeta}{\left[1+(ah)^n\right]^m} + \zeta\left\{1-\left[\frac{\ln(h+1)}{\ln(ho+1)}\right]^{-2}\right\} \qquad (1)$$

where θ is the volumetric water content, θ_{sat} is the saturated θ value, h is the suction (cm), and α, ζ, m, n, and h_0 are fitting parameters. The unsaturated hydraulic conductivity (cm h^{-1}) data were fitted with Campbell's equation:

$$K = K_{sat}\left(\frac{\theta}{\theta_{sat}}\right)^{\omega} \qquad (2)$$

$$\omega = a_k\theta^2 + b_k\theta + c_k \ , \qquad (3)$$

where ω, ak, bk, ck are fitting parameters. The relationship between water content and thermal conductivity (K_h) is given by:

Preprints (www.preprints.org) | NOT PEER-REVIEWED | Posted: 17 August 2018 doi:10.20944/preprints201808.0302.v1

$$K_h = a_h + b_h\left(\frac{\theta}{\theta_{sat}}\right) - (a_h - d_h)\exp\left[-c_h\left(\frac{\theta}{\theta_{sat}}\right)^{\theta e}\right] \tag{4}$$

where a_h, b_h, c_h and d_h are fitting parameters. We estimated these fitting parameters using the method proposed by Campbell (1985) [18] for the surface soil (0–5cm). The estimated thermal conductivity function was verified by comparison with that measured using a thermal conductivity probe (Decagon Devices Inc., Pullman, WA, USA). The same parameter values were used for subsurface soils. The dependence of albedo on the water content (α_R) is given by:

$$\alpha_R = \frac{\alpha_{\max} - \alpha_{\min}}{1 + (a_{al}\bar{\theta}_l)^{b_{al}}} + \alpha_{\min} \tag{5}$$

where θ_l is the average volumetric water content in the top 1 cm (cm^3 cm^{-3}) and $\alpha_{\max}$, $\alpha_{\min}$, α_{al} and β_{al} are fitting parameters. We took measurements using a newly designed device and pyranometer (LI200X Campbell Scientific, Inc) that requires only a small amount of soil sample and allows quick measurement across a wide range of water contents to obtain the parameter values of each soil sample. The accuracy of the values measured using this device was validated using the known data of Fujimaki et al. (2003) [19].

Calibration for simulation of soil hydraulic properties

To verify the accuracy of the predicted water movement, two soil moisture sensors (5TE, Decagon Devices, Inc.) were inserted to monitor the water content, electrical conductivity and temperature at depths of 5 and 15 cm at 3-h intervals, from July 24 to August 8, 2008. Precipitation (ECRN-100, Decagon Devices, Inc) and shortwave radiation (LI200X, Campbell Scientific, Inc) at 3-h intervals were monitored in the same period. Other meteorological data (maximum and minimum temperature, wind velocity and relative humidity) were obtained from IMH. We took core soil samples from depths of 2.5–7.5 and 12.5–17.5 cm from the point where the soil moisture sensors were inserted. Saturated and unsaturated hydraulic properties were measured by the falling head and evaporation methods. Retention data in the high suction range were obtained with the vapor pressure method for surface core samples. We estimated fitting parameters of thermal conductivity and dependence of albedo on the water content using the same method as for the other sampled surface soils. We compared the simulated data of the volumetric water content at depths of 5 and 15 cm using the sampled soil parameters and monitored the values of volumetric water content. The RMSE between simulated and monitored soil water content at depths of 5 and 15 cm were 0.0053 and 0.0181, respectively.

Plant properties

The actual transpiration rate, T, is computed by

$$T = \int S dz \, . \tag{6}$$

The sink term, S (s^{-1}), is defined as the volume of water removed from a unit volume of soil per unit time due to water uptake by a plant, and z is soil depth (cm). Feddes et al. (1978) [20] specified S as

$$S = T_p \beta \alpha_w \, , \tag{7}$$

where T_p, β and α_w are the potential transpiration rate (cm s^{-1}), normalized root density distribution (cm^{-1}) and reduction coefficient, respectively. T_p was given by multiplying the reference evapo-transpiration rate using the Penman equation [21] and crop coefficient (K_c). Kc is expressed as a function of cumulative transpiration:

$$Kc = a_{kc}\left[1-\exp\left(b_{kc}\sum T\right)\right]+c_{kc} \ , \quad (8)$$

where a_{kc}, b_{kc} and c_{kc} are fitting parameters. The values of a_{kc}, b_{kc} and c_{kc} were assumed to be 0.8, -0.4 and 0.3, respectively, based on a previous study [22]. β was given by:

$$\beta = \left(b_{rt}+1\right)d_{_{rt-brt+1}}\left(d_{rt}-z\right)b^{rt} \quad (9)$$

where b is a fitting parameter, and d_{rt} and z are the rooting depth (cm). The value of b was assumed to be unity, based on data from an experiment using these two plants, which means that normalized root density distributions are distributed linearly. The d_{rt} is also expressed as a function of cumulative transpiration:

$$d_{rt} = a_{drt}\left[1-\exp\left(b_{drt}\sum T\right)\right]+c_{drt} \ , \quad (10)$$

where a_{drt}, b_{drt} and c_{drt} are fitting parameters. The values of a_{drt}, b_{drt} and c_{drt} were assumed to be 25, -0.04 and 10, respectively, which means that the rooting depth becomes dipper-shaped depending on cumulative transpiration. These parameter values were adapted by assuming *S. krylovii* and *L. chinensis* have similar rooting depths in the early stage of making a habitat. The α_w was described using the S-shaped function:

$$\alpha_w = \frac{1}{1+(h/h_{50})^p} \quad (11)$$

where h_{50} is the soil water pressure head at which uptake is reduced by half and p is an adjustable parameter. In this work, we set h_{50} = -1302, p = 1.355 and h_{50} = -1254 and p =4.862 for *Stipa krylovii* and *Leymus chinensis*, respectively, given by averaging determined parameters in our previous research [23] (Fig. 1). The parameters were obtained by the pot experiments of full-grown *S. krylovii* and *L. chinensis* (Table 2). Present study, therefore, did not consider about germination process from seed in simulation. Leaf area index (I) was expressed as a function of cumulative transpiration.

$$I = a_{LAI}\left[1-\exp\left(b_{LAI}\sum T\right)\right], \quad (12)$$

where a_{LAI} and b_{LAI} are fitting parameters. Assumed values of a_{LAI} and b_{LAI} were 1 and 0.2, respectively. Parameters related to LAI were assumed based on the results of a previous study in *S. krylovii* and *L. chinensis* dominated grassland [24]. Initial cumulative transpiration was 0.1 cm based on field survey results in Mongolia [25]. Since shortwave radiation flux which arrives at the soil surface is decreased due to vegetation cover, the shortwave flux is expressed as a function of leaf area index. Evaporation rate (*E*) is calculated by a bulk transfer equation as follows:

$$E = \frac{\rho_{vs}h_{rs} - \rho_{va}h_{ra}}{r_a + r_{sc}} \quad (13)$$

where ρ_{vs} is the saturated vapor concentration at the soil surface (g cm^{-3}), ρ_{va} is the saturated vapor concentration at reference height (g cm^{-3}), h_{rs} is the relative humidity at the soil surface (g cm^{-3}), h_{ra} is the relative humidity at reference height, r_a is the aerodynamic resistance (s cm^{-1}) and r_{sc}, is the resistance due to salt crusting (s cm^{-1}). An increase in aerodynamic resistance due to plant cover was also expressed as a function of leaf area index. Vegetation dependent parameters were filled with theoretical values except for h_{50} and p of each species, and each parameter was assumed to be the same value for every numerical experiment.

Preprints (www.preprints.org) | NOT PEER-REVIEWED | Posted: 17 August 2018 doi:10.20944/preprints201808.0302.v1

Table2 Parameter values of plant properties in the simulation

Properties Prameters	*Stipa krylovii*	*Leymus chinensis*
Stress Response Function		
h50	-1302	-1254
a	1.355	4.862
Root Density Distribution		
brt	1	
adrt	25	
bdrt	-0.04	
cdrt	10	
Crop Coefficient		
aKc	0.8	
bKc	-0.4	
cKc	0.3	
Leaf Area Index		
aLAI	1	
bLAI	-0.2	

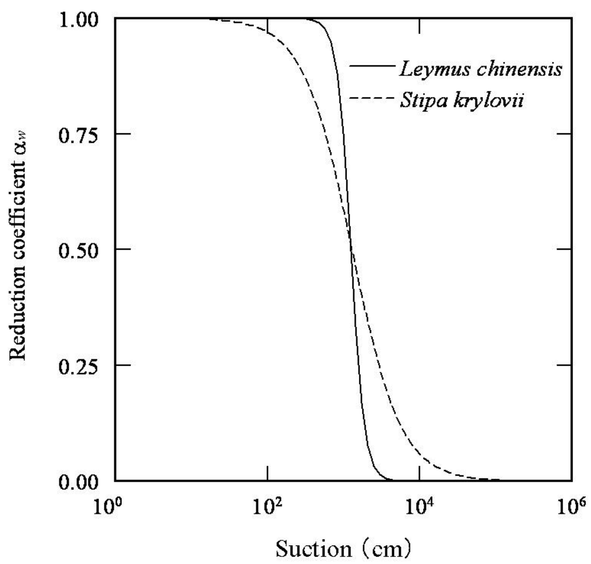

Fig. 1. Drought stress response function for *L. chinensis* and *S. krylovii* applied to the simulations of

Preprints (www.preprints.org) | NOT PEER-REVIEWED | Posted: 17 August 2018 doi:10.20944/preprints201808.0302.v1

water flow in the soil. This response function was the average of the responses of three plants of each plant species.

Particle size distribution

The soil core samples were air-dried and sieved to obtain all particles <2.0 mm after the hydraulic measurements. The particle size distribution for each site was determined using the pipette method.

Results

Particle size distribution and hydraulic properties of surface soil samples

The average particle size distribution of soils at the different sampled sites is shown in Table 3. The coarse sand content was highest at the CA2 site, and its fine sand content was higher than at the cropland sites abandoned for longer periods. The fine sand content at the SNG site was the highest of all sites.

Figures 2 and 3 show the unsaturated hydraulic conductivity and water retention curves for the surface soils at the four sites. The unsaturated hydraulic conductivity of soils from abandoned fields, especially at the CA2 site, was higher than that for the soil at the SNG site at a given volumetric water content. The suction of the soil from abandoned fields at the CA2 site was lower than that for the soil at the SNG site at a given volumetric water content (ex. volumetric water content is 0.2 cm^3 cm^{-3}). Suction values for soils at the CA9 and CA18 sites fell between values from the CA2 and SNG sites.

Table 3 Particle size distribution of soils at the study sites.

	Particle size distribution (%)			
Site	Clay (<0.002mm)	Silt (0.002-0.02mm)	Fine sand (0.02-0.25mm)	Coarse sand (0.25-2.00mm)
CA2	11.15 (±2.76)	23.70 (±3.94)	34.12 (±5.75)	31.03 (±3.64)
CA9	17.25 (±1.13)	31.15 (±6.09)	38.68 (±3.04)	12.91 (±5.55)
CA18	13.88 (±4.54)	19.22 (±3.24)	45.90 (±6.47)	21.00 (±3.04)
SNG	10.17 (±1.75)	25.08 (±1.18)	46.84 (±4.48)	17.91 (±4.05)

( ) values show the standard error.

Preprints (www.preprints.org) | NOT PEER-REVIEWED | Posted: 17 August 2018 doi:10.20944/preprints201808.0302.v1

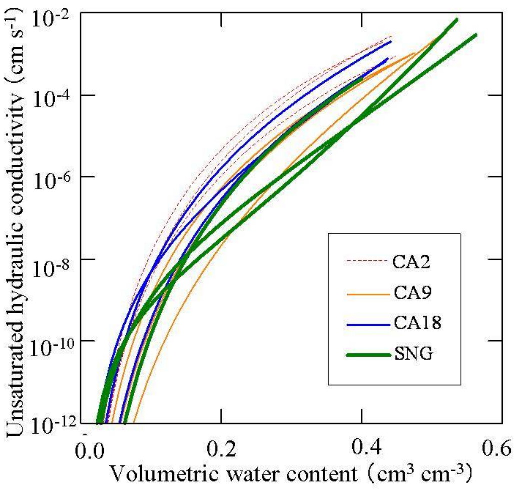

Fig. 2. Unsaturated hydraulic conductivity of soil samples at depths of 0–5 cm as a function of the volumetric water content. Three replications were measured for each site: curves of the same style represent values from the same site.

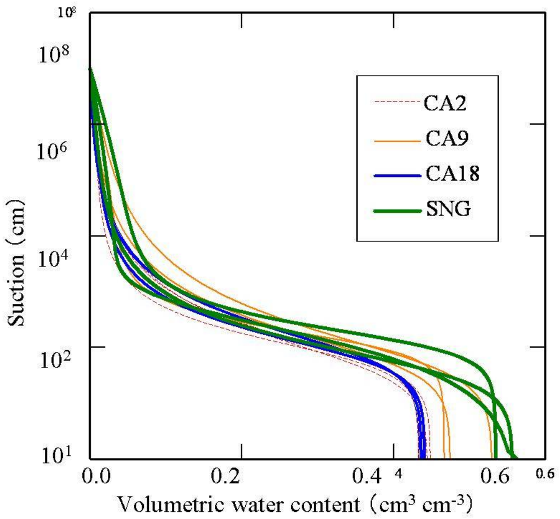

Fig. 3. Soil water-retention curves for soil samples at depths of 0–5 cm from the four sites: suction as a function of the volumetric water content. Three replications were measured for each site: curves of the same style represent values from the same site.

 doi:10.20944/preprints201808.0302.v1

Volumetric water content and soil water suction in drought and non-drought summers

Figure 4 shows the average volumetric water content of surface soils from the different sampled sites in the summer of drought and non-drought years. There are no obvious differences among sites. Figure 5 shows changes in soil suction in the same years. There were large differences in terms of suction in the surface soil. Soil suction in abandoned fields was lower than that at the SNG site, and at the CA2 site, was the lowest of all sites in the drought year. Although there was not a large difference in suction between the CA9- and CA18 sites in the non-drought year (Fig. 4a), the suction at the CA18 site was higher than that at the CA9 site in the drought year (Fig. 4b). Thus the difference in suction in the surface soil in the drought summer was larger than in the non-drought year. In the sub-surface soil, there were no obvious differences in suction among the sites for both the drought and non-drought years.

 doi:10.20944/preprints201808.0302.v1

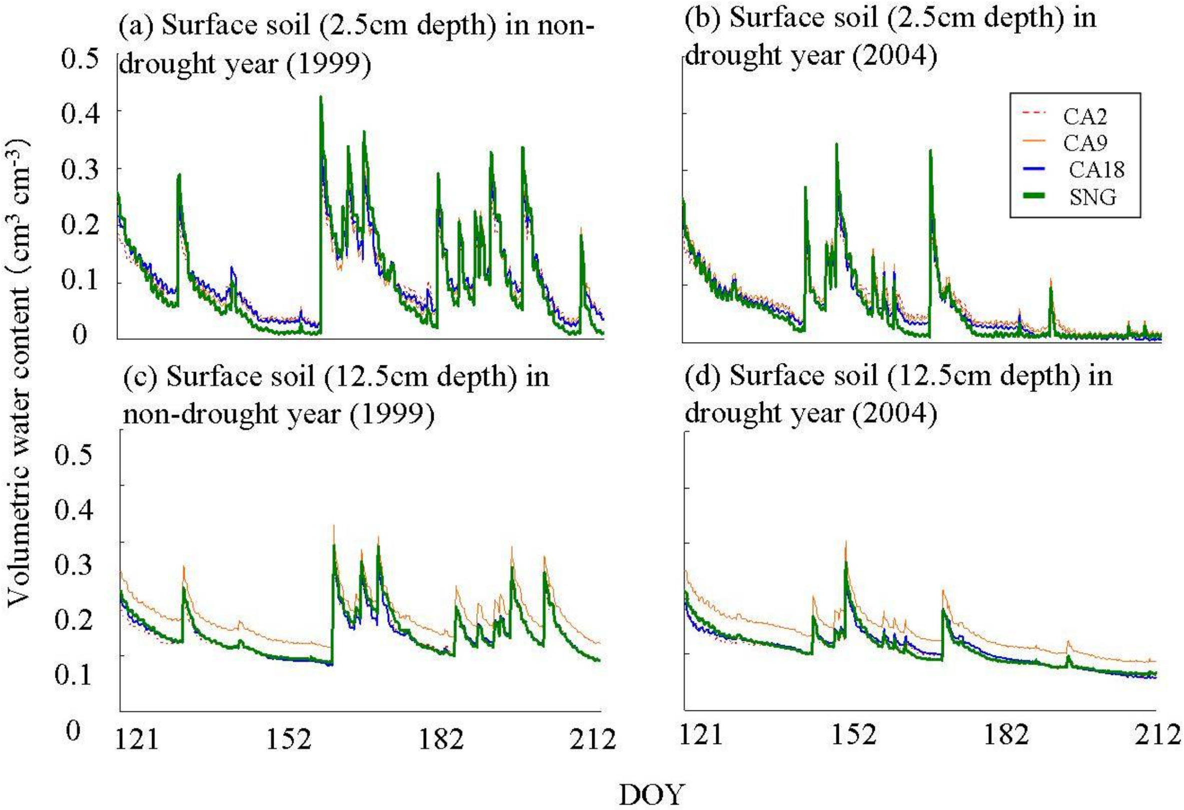

Fig. 4. Volumetric water content at depths of 2.5 and 12.5 cm at each site in non-drought (1999) and drought (2004) summers. Each value is the average of three samples.

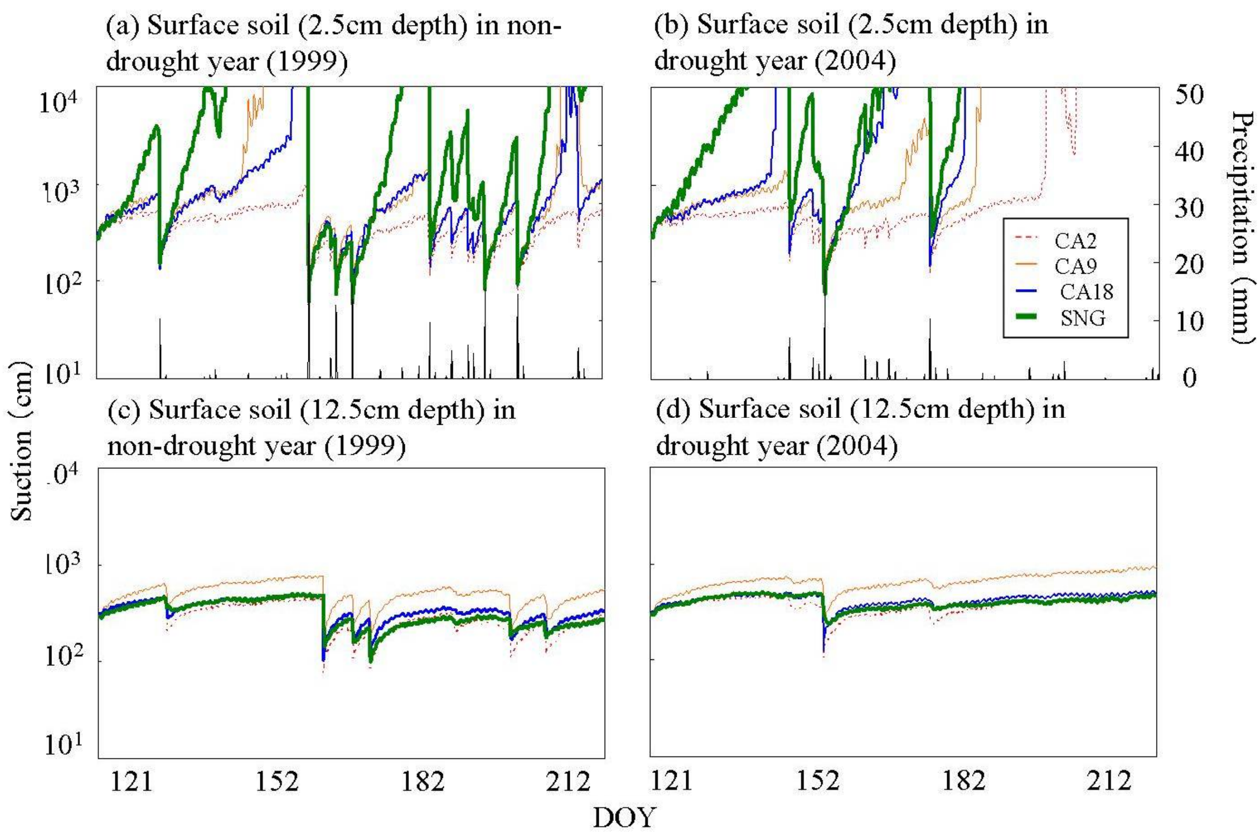

Fig. 5. Soil water suction at depths of 2.5 and 12.5 cm at each site in non-drought (1999) and drought (2004) summers. Each value is the average of three samples.

Cumulative transpiration of *L chinensis* and *S. krylovii* and soil water suction in drought and non-drought summers and average cumulative transpiration are shown in Figure 6. The bar graphs show the cumulative transpiration at the end of July (DOY = 212). The cumulative transpiration of *L. chinensis* was slightly higher than that of *S. krylovii* in the non-drought year at all three sites. In contrast, the cumulative transpiration of *S. krylovii* was slightly higher than that of *L. chinensis* in the drought year at all three sites.

 doi:10.20944/preprints201808.0302.v1

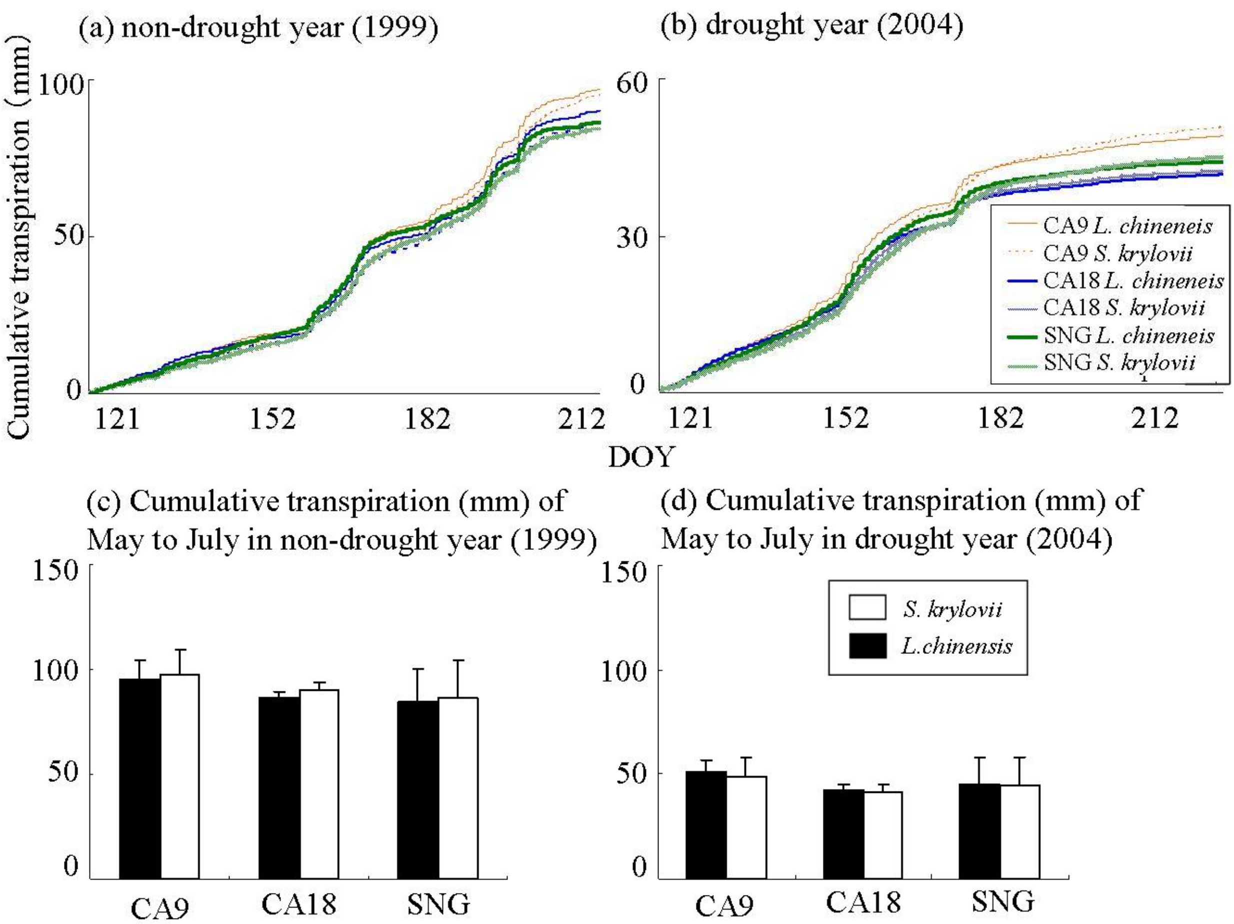

Fig. 6. Cumulative transpiration of *L.chinensis* and *S. krylovii* at the CA9, CA18 and SNG sites in non-drought (1999) and drought (2004) summers. Each value is the average of three samples.

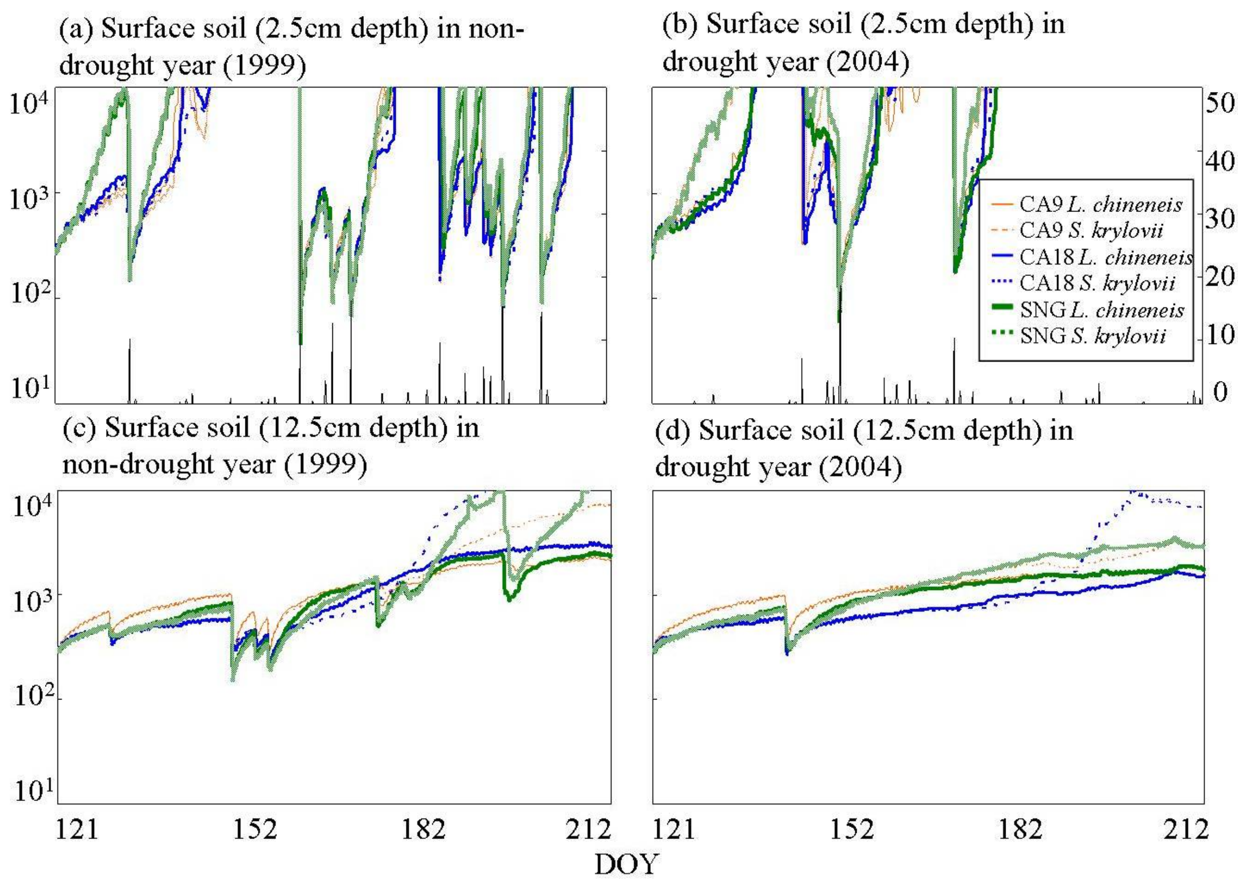

Fig. 7. Soil water suction at depths of 2.5 and 12.5 cm at each site under growth of *L. chinensis* and *S. krylovii* in non-drought (1999) and drought (2004) summers. Each value is the average of three samples.

Figure 7 shows that the suction of subsurface soils under growing *S. krylovii* was higher than that under *L. chinensis* in the drought year. Meanwhile, the soil suctions of surface and subsurface soils under the growing *S. krylovii* were higher than that under *L. chinensis* in the drought year.

Discussion

Particle size distribution and hydraulic properties of surface soil samples

The difference in particle size distribution among sites seems to be related to dust storms and differences in vegetation at these sites. More than half of the dust storms in Mongolia occur in the spring [26], a season when perennial species begin to grow in the grasslands. In contrast, the ground remains essentially bare in spring in areas dominated by annual species in early stage abandoned croplands (for example the CA2 site). Therefore, a greater amount of soil erosion may occur in areas with sparse vegetation [26]. Consequently, we suggest that the fraction of coarse sand that is less easily transported by dust storms owing to its size and weight remains, and the fraction of fine sand that is easily carried away might have decreased at the CA2 site. Since fine sand is easily trapped around vegetation due to its weight during wind storms, there is a possibility that it concentrates in springtime in fields with perennial species [27,28], such as the CA18 and SNG sites.

The unsaturated hydraulic conductivity and suction of the soils at the SNG site at a given water content were the lowest and highest of all sites, respectively. This means that soil water at the SNG site will move though the soil micro-structure slowly due to the high suction of the capillary force in soil micro pores in this structured soil [1,29]. On the other hand, the soil structure of abandoned fields such as in CA2 has been largely destroyed by past tillage and has lost its fine sand content due to wind erosion. Therefore, the soil in abandoned fields was less structured in comparison with the SNG site.

It has been reported that the volume fraction of capillary pores for available water for plants and macro pores in an abandoned cropland was lower and higher, respectively, than those in grassland without a history of cultivation, because of destruction of the soil structure by past tillage [1]. Soil water in abandoned fields, such as CA2, is retained in macropores at low suction. Consequently, the suction in abandoned fields, especially in CA2, is lower than in SNG at a given volumetric water content.

Volumetric water content and suction of soil water in drought and non-drought summers

The lower content of coarse sand may lead to higher soil suction at the SNG site and at the later stage of abandoned fields, CA18, which may affect suction of the surface soil at each site after rainfall (Fig. 4a and 4b). The structured soil which has a lower coarse sand content and many capillary pores contributed to keeping the water at high suction. On the other hand, soil water at the CA2 site was retained in developing macropores consisting of coarse sand, whose size is too large to maintain a high capillary force. The differences in surface soil suction among the sites implie a difference in land-use history and periods of abandonment. The present study suggests that surface soil suction more clearly indicated soil hydraulic conditions for plant growth than the volumetric water content. Suction in the surface soils seems to indicate that the available water is restricted for drought tolerant plants at the CA18 and SNG sites and is less restricted at the CA2 site.

There were few differences in the volumetric water content and suction in the subsurface

Preprints (www.preprints.org) | NOT PEER-REVIEWED | Posted: 17 August 2018 doi:10.20944/preprints201808.0302.v1

soils among sites except for the CA9 site. The high value of *Wsat* of CA9a and CA9c (Table 1) results in the differences in the volumetric water content and soil water suction observed at the CA9 site. The volumetric water content and suction in the subsurface soil were relatively more abundant (Fig. 3c and d) and lower (Fig. 4c and d) than in the surface soil, respectively. In general, the root depth of perennial species is deeper than for annual species, and the growth rate of perennial species relies on subsurface soil water. Therefore, the high suction of the surface soil at the CA18 and SNG sites has less possibility of preventing the growth of perennial species.

Although previous studies have shown changes in water retention curves and hydraulic conductivities of the near-saturated range of surface and subsurface soils [12,13] and of the unsaturated range (i.e., high suction range) of surface soils [1] due to crop abandonment, the present study indicates that suction of the surface soil water differed according to the period of abandonment and climatic conditions considering infiltration into and capillary rise from the subsoil.

Cumulative transpiration of *L chinensis* and *S. krylovii* and soil water suction in drought and non-drought summers

The higher cumulative transpiration of *L. chinensis* occurred in the days immediately following rainfall (e.g. Fig. 6a, DOY: 195) in the non-drought year, which may be caused by a difference in the reduction coefficient at around -1000 cm (Fig. 1). *Leymus chinensis* can maintain its potential transpiration rate up to a suction of about -1000 cm. This variation of cumulative transpiration along with the weather conditions shows why *L. chinensis* is the predominant species in habitats with relatively abundant water [30]. *L. chinensis* seemed to retain its advantage in transpiration at places with abundant water due to its drought tolerance at relatively low suction.

The cumulative transpiration of *S. krylovii* was higher than that of *L. chinensis* at every site in the drought year of 2004 (Fig. 6d). Since *S. krylovii* has tolerance to drought stress at relatively high suctions (Fig. 1), it seems to contribute to the higher cumulative transpiration for *S. krylovii* in drought years. *Stipa krylovii* decreased its transpiration rate under conditions of relatively low drought stress, but it retained a low transpiration rate under relatively high drought stress conditions (h > 1000cm) (Fig. 1). In a drought year, *S. krylovii* may use its drought tolerance at relatively high suction and replace *L. chinensis*. *Stipa krylovii* was observed at the CA18 and SNG sites where suction increases relatively quickly after rainfall (Fig. 5), which may indicate a possible advantage of *S. krylovii* and its replacement at the CA18 and SNG sites in a drought year. Shinoda et al. (2010) reported that *L. chinensis* diminished their above-ground biomass following a two year drought, but *S. krylovii* did not decrease its biomass even after a third year of drought. The present study suggests a reason for the tolerance of *S. krylovii* to continuous drought.

The soil water suction at a depth of 2.5 cm under *S. krylovii* was higher than that of *L. chinensis* at each site in the drought year (Fig. 5b). Therefore, soil conditions in terms of suction under the *S. krylovii* community seem harsh in terms of water uptake by other plant species in a drought year. Shinoda et al. (2010) [3] showed that most of the annual species did not grow in a mixed community of perennial and annual species in drought conditions, which may be due to the relatively high soil water suction in the surface soil aggravated by drought tolerant species such as

S. krylovii. Since annual species are dependent on the soil water in the surface layer, lack of available soil water in the surface is critical for them. These phenomena may indicate a competitive superiority of *S. krylovii* in dry Mongolian rangeland.

In abandoned cropland, the typical dry soil conditions were lost due to an increase in the fraction of coarse sand, especially at the CA2 site. The soil water is retained in the macropores at low suction (power), which means that this soil water could be used more easily than water at higher suction in the capillary pores, because soil water at low suction is preferred by annual plants. In these abandoned croplands, typical perennial grasses, such as *S. krylovii* which has a tolerance for relatively high drought stress, would not have an advantage in this non-dry soil condition. In contrast, the increase in fine sand content of the surface soil layer with increasing period of abandonment and irregular drought would contribute to providing dry conditions and encourage the replacement of *L. chinensis* by *S. krylovii*. The present study suggests the importance of typical dry conditions of soil and climate for the growth of the typical perennial grass, *S. krylovii*, in degraded abandoned fields. This abiotic interaction between soil hydraulic properties and climate conditions appears to play an important role in plant succession in abandoned cropland.

Acknowledgments

This study would not have been possible without the willing cooperation of the staff of Hustai National Park. We sincerely thank them all, especially Prof. B. Namkhai (Director, Hustai National Park). We also thank assistant professor S. Okubo and Dr. T. Okayasu (Department of

 doi:10.20944/preprints201808.0302.v1

Ecosystem Studies, Graduate School of Agricultural and Life Sciences, The University of Tokyo) for their helpful comments. This study was conducted under the Global Environmental Research Fund of Japan's Ministry of the Environment “Desertification Control and Restoration of Ecosystem Services in Grassland Regions of North-East Asia” (no. G-071), with the additional support of a JSPS Research Fellowship for Young Scientists awarded to A. Yanagawa (no. 20-7002 and 24-7604).

References

1. Hoshino, A.; Tamura, K.; Fujimaki, H.; Asano, M.; Ose, K.; Higashi, T. Effects of crop abandonment and grazing exclusion on available soil water and other soil properties in a semi-arid mongolian grassland. *Soil and Tillage Research* **2009**, *105*, 228-235.
2. Zhao, W.Z.; Xiao, H.L.; Liu, Z.M.; Li, J. Soil degradation and restoration as affected by land use change in the semiarid bashang area, northern china. *CATENA* **2005**, *59*, 173-186.
3. Shinoda, M.; Nachinshonhor, G.U.; Nemoto, M. Impact of drought on vegetation dynamics of the mongolian steppe: A field experiment. *J. Arid Environ.* **2010**, *74*, 63-69.
4. Zhan, X.; Li, L.; Cheng, W. Restoration of *stipa krylovii* steppes in inner mongolia of china: Assessment of seed banks and vegetation composition. *J. Arid Environ.* **2007**, *68*, 298-307.
5. Swiss Agency for Development and Cooperation, S. *“Green gold” pasture ecosystem management program*; Ulaanbaatar, 2009; pp 12-13.
6. Hoshino, A.; Yoshihara, Y.; Okuro, T.; Undarmaa, J.; Takeuchi, K. Effects of vegetation gap on subsequent species richness and cover on abandoned cropland in semi-arid grasslands of mongolia. *Sand Dune Research* **2009**, *56*, 29-38.
7. Hobbs, R.; Harris, J. Restoration ecology: Repairing the earth's ecosystems in the new millennium. *Restor. Ecol.* **2001**, *9*, 239-246.
8. Kosmas, C.; Gerontidis, S.; Marathianou, M. The effect of land use change on soils and vegetation over various lithological formations on lesvos (greece). *CATENA* **2000**, *40*, 51-68.
9. Xu, Z.; Wan, S.; Zhu, G.; Ren, H.; Han, X. The influence of historical land use and water availability on grassland restoration. *Restor. Ecol.* **2010**, *18*, 217-225.
10. Bonet, A.; Pausas, J. Species richness and cover along a 60-year chronosequence in old-fields of southeastern spain. *Plant Ecol.* **2004**, *174*, 257-270.
11. Li, Y.Y.; Shao, M.A. Change of soil physical properties under long-term natural vegetation

restoration in the loess plateau of china. *J. Arid Environ.* **2006**, *64*, 77-96.
12. Ahuja, L.R.; Fiedler, F.; Dunn, G.H.; Benjamin, J.G.; Garrison, A. Changes in soil water retention curves due to tillage and natural reconsolidation. *Soil Sci. Soc. Am. J.* **1998**, *62*, 1228-1233.
13. Schwartz, R.C.; Evett, S.R.; Unger, P.W. Soil hydraulic properties of cropland compared with reestablished and native grassland. *Geoderma* **2003**, *116*, 47-60.
14. FAO/ISRIC/ISSS. *World reference base for soil resources*. FAO: Rome, 1998.
15. Bowman, R.A.; Reeder, J.D.; Lober, R.W. Changes in soil properties in a central plains rangeland soil after 3, 20, and 60 years of cultivation. *Soil Science* **1990**, *150*, 851-857.
16. Šimůnek, J.; Wendroth, O.; Van Genuchten, M. Parameter estimation analysis of the evaporation method for determining soil hydraulic properties. *Soil Sci. Soc. Am. J.* **1998**, *62*, 894-904.
17. Fujimaki, H.; Inoue, M. Reevaluation of the multistep outflow method for determining unsaturated hydraulic conductivity. *Vadose Zone Journal* **2003**, *2*, 409-415.
18. Campbell, G. *Soil physics with basic: Transport models for soil-plant systems*. Elsevier Science Ltd: New York, 1985.
19. Fujimaki, H.; Shiozawa, S.; Inoue, M. Effect of salty crust on soil albedo. *Agricultural and Forest Meteorology* **2003**, *118*, 125-135.
20. Feddes, R.A.; Kowalic, P.J.; Zaradny, H. *Simulation of field water use and crop yield.* Jon Wiley & Sons: New York, 1978.
21. Hillel, D. *Environmental soil physics*. Academic Press: 1998.
22. Hou, Q.; Wang, Y.; Yang, Z.; Shi, G. Dynamic simulation and definition of crop coefficient for typical steppe in inner mongolia, china. *Chinese Journal of Plant Ecology* **2010**, *34*, 1414-1423.
23. Yanagawa, A.; Fujimaki, H.; Okuro, T.; Jamsran, U.; Takeuchi, K. Comparison of drought tolerances in root water uptake model for two co-occuring grass species in mongolia. *Journal of the Japanese Society of Soil Physics* **2015**, *130*, 3-10.
24. Wang, R.; Chen, L.; Bai, Y.; Xiao, C. Seasonal dynamics in resource partitioning to growth and storage in response to drought in a perennial rhizomatous grass, *leymus chinensis*. *J. Plant Growth Regul.* **2008**, *27*, 39-48.
25. Matsuura, Y. Estimation of evapotranspiration and land-cover with satellite data in semi-arid mongolia. Tohoku University, 2004.
26. Natsagdorj, L.; Jugder, D.; Chung, Y.S. Analysis of dust storms observed in mongolia during 1937-1999. *Atmos. Environ.* **2003**, *37*, 1401-1411.
27. Lancaster, N.; Baas, A. Influence of vegetation cover on sand transport by wind: Field studies at owens lake, california. *Earth Surface Processes and Landforms* **1998**, *23*, 69-82.
28. Liu, L.Y.; Li, X.Y.; Shi, P.J.; Gao, S.Y.; Wang, J.H.; Ta, W.Q.; Song, Y.; Liu, M.X.; Wang, Z.; Xiao, B.L. Wind erodibility of major soils in the farming-pastoral ecotone of china. *J. Arid Environ.* **2007**, *68*, 611-623.

29. Hoshino, A. Physico-chemical properties and micromorphological characteristics of the soils under grazing and cultivated fields in the kherlen river basin, mongolia. University of Tsukuba, Tsukuba, 2006.
30. Chen, S.; Bai, Y.; Zhang, L.; Han, X. Comparing physiological responses of two dominant grass species to nitrogen addition in xilin river basin of china. *Environ. Exp. Bot.* **2005**, *53*, 65-75.